CHEMISTRY
A European Journal

A Journal of
ChemPubSoc Europe

Accepted Article

Title: Cellular Target of a Rhodium Metalloinsertor is the DNA Base Pair Mismatch

Authors: Kelsey M. Boyle, Adela Nano, Catherine Day, and Jacqueline K. Barton

To be cited as: *Chem. Eur. J.* 10.1002/chem.201900042

Link to VoR: http://dx.doi.org/10.1002/chem.201900042

Supported by
ACES

WILEY-VCH

10.1002/chem.201900042

WILEY-VCH

COMMUNICATION

Cellular Target of a Rhodium Metalloinsertor is the DNA Base Pair Mismatch

Kelsey M. Boyle, Adela Nano, Catherine Day, and Jacqueline K. Barton*

Abstract: Defects in DNA mismatch repair (MMR) are commonly found in various cancers, especially in colorectal cancers. Despite the high prevalence of MMR-deficient cancers, mismatch-targeted therapeutics are limited and diagnostic tools are indirect. Here, we examine the cytotoxic properties of a rhodium metalloinsertor, $[Rh(phen)(chrysi)(PPO)]^{2+}$ (**RhPPO**) in 27 diverse colorectal cancer cell lines. Despite the low frequency of genomic mismatches and the non-covalent nature of the **RhPPO**-DNA lesion, **RhPPO** is on average 5 times more potent than cisplatin. Importantly, the biological target and profile for **RhPPO** differs from that of cisplatin. A fluorescent metalloinsertor, **RhCy3**, was used to demonstrate that the cellular target of **RhPPO** is the DNA mismatch. **RhCy3** represents a direct probe for MMR-deficiency and correlates directly with the cytotoxicity of **RhPPO** across different cell lines. Overall, our studies clearly indicate that **RhPPO** and **RhCy3** are promising anticancer and diagnostic probes for MMR-deficient cancers, respectively.

Deficiencies in cellular mismatch repair (MMR) machinery are a hallmark of 14% of colorectal cancer cases and up to 20% of all solid tumors.[1,2] Cells with MMR-deficiencies (MMR−) cannot repair DNA mismatches or insertions/deletions (indels), leading to a relative abundance of these lesions in these cells. Mismatches could thus serve as a unique druggable target that has yet to be utilized in a clinical setting. Furthermore, these lesions could serve as a target for direct detection and diagnosis of MMR deficiencies in tumors, something that is commonly measured indirectly through tests of mutational frequency in microsatellite regions instead of number of mismatches.[2b] Such a diagnostic would further support the promise of a mismatch- and indel-targeted therapeutic agent. Our group and others have addressed this need through the development of mismatch-targeted small molecules.[3] Specifically, our group has developed a unique family of metal complexes, called rhodium metalloinsertors, that can selectively target thermodynamically destabilized regions of DNA, such as base pair mismatches (Figure 1), small indels, and abasic sites, making the metal complexes an ideal candidate for targeting and detecting the DNA lesions found in MMR-deficient tumors.[4–7]

Rhodium metalloinsertors have been rigorously studied in several pairs of matched cancer cell lines which differ primarily in the presence or absence of functioning MMR machinery.[8,9] In every matched pairing, metalloinsertors are significantly more cytotoxic towards the MMR− cell line compared to their MMR-proficient (MMR+) counterpart (a feature referred to as selectivity). These results demonstrate that rhodium metalloinsertors can target MMR deficiencies in cells, however they do not prove the specific cellular target of metalloinsertors to be DNA mismatches. Furthermore, these cell pairings are not reflective of the diversity of clinical colorectal cancer (CRC) cases; in reality, the differences between tumors in two different patients or healthy and cancerous tissues in a single patient will be far greater than just the presence or absence of a single MMR protein.[10,11]

[a] K. M. Boyle, Dr. A. Nano, C. Day, Prof. J. K. Barton
Division of Chemistry and Chemical Engineering
California Institute of Technology
1200 East California Boulevard, MC 127-72, Pasadena, California 91125 (USA)
Email: jkbarton@caltech.edu

Supporting information for this article is given via a link at the end of the document.

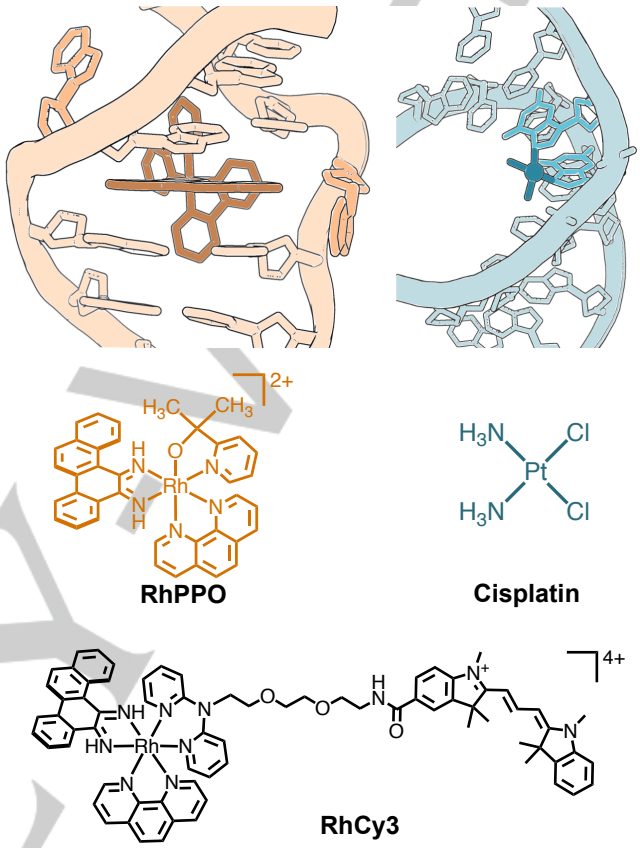

Figure 1. The binding and structure of a metalloinsertor and cisplatin. As observed crystallographically in previous studies, a classic metalloinsertor binds selectively to a mismatch in DNA (top left, PDB 3GSK), while cisplatin binds to a d(GpG) site in DNA (top right, PDB 1AIO). The structures of **RhPPO** (middle left), cisplatin (middle right), and **RhCy3** (bottom).

To understand more fully the potential clinical applicability of rhodium metalloinsertors, we examined our most potent and selective metalloinsertor, $[Rh(phen)(chrysi)(PPO)]Cl_2$ (**RhPPO**, Figure 1), across 27 CRC cell lines (Table S1).[12,13] These cell lines represent a diverse set of tumors, spanning the four subtypes of CRC and both MMR− and MMR+ phenotypes.[14,15] The toxicities of **RhPPO**, which selectively targets MMR deficiencies, and the non-selective FDA-approved chemotherapeutic cisplatin, which covalently binds the abundant d(GpG) motifs present in all DNA (Figure 1), were assessed in this cell line panel using a luciferase-based luminescence assay which measures ATP from living cells. Dose-response curves and corresponding IC50 values (50% inhibitory concentration) were determined for each therapeutic and are shown in Figure 2 and Table S2. The IC50 values of **RhPPO** in different cell lines span nearly three orders of magnitude, ranging from 63 ± 3 nM to 18 ± 3 μM. Despite the low number of genomic mismatches, **RhPPO** is more potent than cisplatin in nearly every cell line, with the IC50 values of **RhPPO** being on average 5 times lower than those of cisplatin (2.9 μM vs. 13.2 μM, respectively). This result is remarkable considering that DNA mismatches are significantly less abundant than d(GpG) sites and metalloinsertors interact only through non-covalent stacking with these mismatches. The potency of a therapeutic in cell culture has long been considered

10.1002/chem.201900042

a key predictor of its clinical success; potent therapeutics have the potential for low dosing conditions,

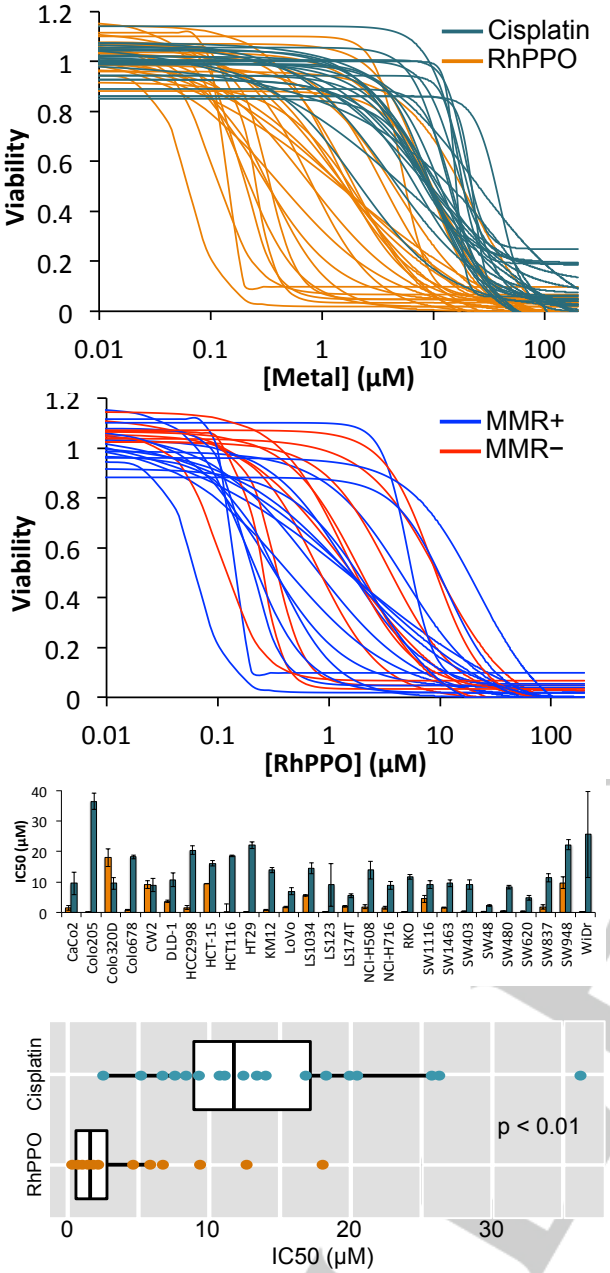

Figure 2. Cytotoxicity of **RhPPO** and cisplatin in 27 colorectal cancer cell lines. Dose response curves of **RhPPO** and cisplatin in CRC cell lines (top). Dose response curves of **RhPPO** in MMR− and MMR+ CRC cell lines (middle top). Direct IC50 comparison of **RhPPO** and cisplatin in 27 CRC cell lines (middle bottom) and boxplot representation, with an average IC50 for **RhPPO** of 3.02 μM and a median of 1.34 μM, and an average IC50 for cisplatin of 13.89 μM and a median of 11.62 μM (bottom).

low off-target effects, and minimal solubility issues.[16,17] Therefore, the high potency of **RhPPO** highlights its great therapeutic potential. Furthermore, in the cell lines least sensitive to cisplatin (Colo205, HT29, and WiDr), **RhPPO** is over 100 times more potent than cisplatin (Table S2), suggesting it could be a particularly useful therapeutic for treatment of clinically challenging cisplatin-resistant tumors.

When considering MMR status, a wide range of sensitivities is observed for both MMR− and MMR+ cell lines (Figure 2). The sensitivities of some cell lines are contrary to what we expected based solely on MMR status; some MMR− cell lines (DLD-1, HCT15, and CW2) show minimal sensitivity to **RhPPO**, whereas some MMR+ cell lines (HT29, WiDr, Ls123, and Colo205) show high sensitivity to **RhPPO**. Overall **RhPPO** shows moderate selectivity towards the MMR− cell lines (average IC50 of 2.5 μM) compared to MMR+ cell lines (average IC50 of 3.0 μM), and the selectivity increases further when looking only at cell lines with deficiencies in MLH1 or MSH2, the two most essential MMR proteins (average IC50 of 2.1 μM, Figure S1). These results are promising and follow the expected trend, however they are not as significant as anticipated (Figure S1). The range observed for both MMR− and MMR+ cell lines can be rationalized; unlike in matched cell lines, cell lines in this panel differ in mutations and regulation of many proteins.[10,11] Accordingly, there are several factors that could obscure the strong MMR− selectivity we expected based on our hypothesis. We investigated two such factors that seemed likely to influence metalloinsertor toxicity: cellular uptake and the number of lesions in genomic DNA that can be targeted by metalloinsertors.

Cell lines can exhibit different uptake and efflux properties towards small molecule therapeutic, therefore differences in uptake between cell lines may explain the wide cytotoxicity range of **RhPPO**.[18,19] We measured the whole cell uptake of **RhPPO** after 24 hours in various cell lines by ICP-MS to determine if the whole cell uptake of **RhPPO** correlated with cytotoxicity (Figure 3 and Figure S2). A significant correlation (Pearson's r = -0.63, $p < 0.01$) was observed between increasing **RhPPO** uptake and decreasing IC50. Furthermore, several of the results contrary to our hypothesis (i.e. high IC50 in MMR− cells, low IC50 in MMR+ cells) are clarified by this assay; the three MMR− cell lines least sensitive to **RhPPO** (DLD-1, HT29, CW2) show the lowest cellular uptake and two of the most sensitive MMR+ cell lines (Ls123 and Colo205) exhibit the highest cellular uptakes. For these cell lines, high or low cellular uptake of **RhPPO** likely obscures the selectivity that would normally be observed on the basis of MMR status alone. While this correlation between uptake and cytotoxicity is intuitive, it is of note that there are few reported studies correlating cellular uptake and cytotoxicity of a small molecule therapeutic across different cell lines.[20] More commonly, reports examine the correlation of cellular uptake and cytotoxicity of different therapeutics in a single cell line or look only at a relatively small number of cell lines.[21] Therefore, our results comparing cytotoxicity and cellular uptake suggest that uptake may often play a non-negligible role in the cytotoxicity differences of a small molecule therapeutic between cell lines.

While a correlation between cytotoxicity and uptake is expected for any small molecule therapeutic, a correlation between cytotoxicity and DNA binding would only be expected if DNA were the relevant biological target of the therapeutic being studied. As discussed previously, inactivation of MMR proteins confers the cells with an increased level of uncorrected mismatches and indels that propagate into mutations upon replication.[3] The number of these lesions in the genome can fluctuate between cell lines, for instance mutations (an indirect measure of mismatches and indels) occur at different rates in cell lines deficient in different MMR proteins.[22] The number of these lesions present in the genomic DNA (gDNA) of a cell could influence differences in potency of **RhPPO**, which targets these destabilized DNA features, in different cell lines.[5,7] Currently, there are few techniques developed for the detection and sensitive measurement of destabilized lesions in gDNA, such as polymerase chain reaction (PCR) amplification, but these techniques are destructive and time-consuming.[23] Fluorescence-based probes have been widely used to visualize and quantify dynamic processes in live cells via interaction with various biological targets and are great candidates for screening of damaged DNA.[24]

10.1002/chem.201900042

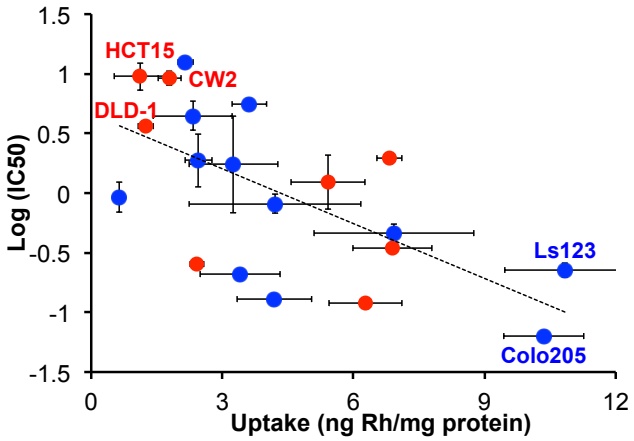

Figure 3. A correlation between whole cell uptake and IC50 for **RhPPO**. A correlation of −0.63 is observed. MMR− cell lines are shown in red and MMR+ are shown in blue, with select cell lines labeled.

As such, our group recently reported a bifunctional fluorescent probe, **RhCy3**, which exhibits a fluorescent light-up effect upon interaction with thermodynamically destabilized mismatches in gDNA (Figure 1).[25] The fluorescence of **RhCy3** is an exceptional readout on the relative number of destabilized lesions in gDNA and an excellent predictor of the relative number of targetable DNA lesion for **RhPPO**, which is structurally similar.

Here we use this probe to better understand the cytotoxic effect of **RhPPO** on a panel of cancer cell lines, but these studies also demonstrate the powerful detection and diagnostics properties of **RhCy3** in MMR− cancers. We performed fluorescence titrations with **RhCy3** and increasing amounts of gDNA extracted from a test set of eight cell lines that span deficiencies in different MMR genes (Table S2).[26] As can be seen in Figure 4, a correlation (r = -0.52) was observed between increasing **RhCy3** fluorescence and decreasing IC50 of **RhPPO**. By removing the potential outlier, DU145 (the only cell line tested mutated in two MMR proteins), the correlation improves dramatically, (r = -0.81, p <0.05), suggesting other factors may influence the cytotoxicity of **RhPPO** or fluorescence of **RhCy3** in DU145. This strong correlation between the IC50 of **RhPPO** and the fluorescence of the reporter **RhCy3** confirms that the effective biological target of rhodium metalloinsertors is, in fact, DNA lesions such as mismatches and indels, and that differences in the number of these lesions between different cell lines controls cytotoxicity of metalloinsertor therapeutics. Notably, there is a clear relationship between the identity of MMR protein and **RhCy3** fluorescence output, showing **RhCy3** can serve as a direct detection method of destabilized lesions in mismatch-repair deficient tumors and a potential diagnostic for these cancers (Supplemental Discussion and Figure S3).

The results presented here highlight some interesting considerations for in vitro studies performed in any laboratory. We observed a large range of IC50 values spanning nearly three orders of magnitude for a single small molecule therapeutic across 27 cell lines. This result alone has significant implications for in vitro experiments. Many studies examine a therapeutic of interest in a single cell line or one cell line from several types of cancer (colorectal, ovarian, etc.), but a single cell line cannot represent cancer or any subtype of cancer as a whole. It is also common to compare cytotoxicity in unmatched cell lines that differ in the expression level of a protein of interest (regular expression, overexpression, and underexpression). Our results here suggest that using only a small number of unmatched cell lines may produce misleading results. For example, in this study we could consider MMR+ cells to have regular MMR expression and MMR− to underexpress MMR proteins. If we randomly chose only two cell lines from our panel, one MMR+ and one

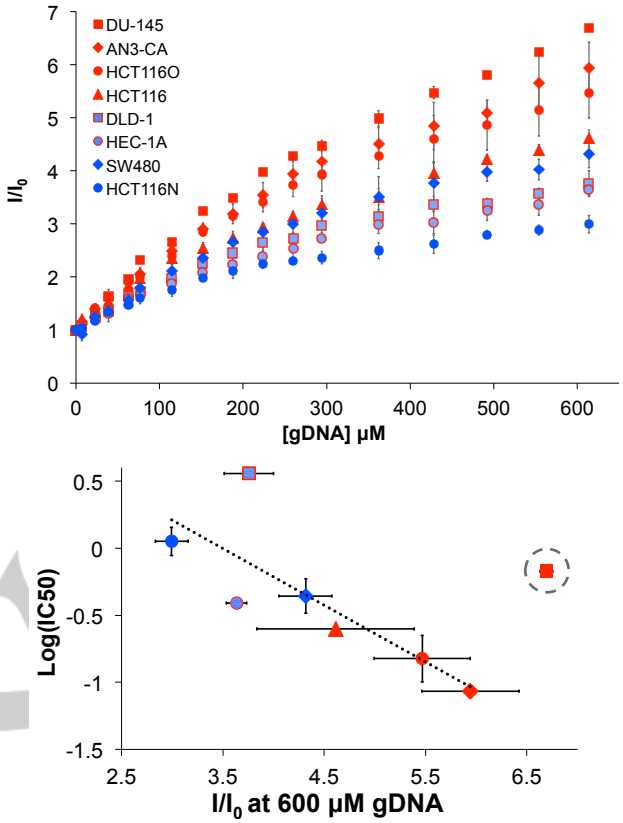

Figure 4. **RhCy3** fluorescence assay with gDNA. Full fluorescence titrations of gDNA extracted from eight different cancer cell lines, with [gDNA] as per base pairs, I as the emission integral from 548 – 675 nm as scalar function measured after each addition of DNA, and I_0 is the emission integral of **RhCy3** solution without gDNA (top). Correlation of r = −0.52 is observed between IC50 value and max I/I_0 for all cell lines (bottom). Removal of a potential outlier (circled) leads to correlation of r = −0.81 between IC50 value and max I/I_0 for all cell lines.

MMR−, we could observe every possible trend. Comparing RKO (MMR−, IC50: 120 nM) and Colo320DM (MMR+, IC50: 18.0 μM) would suggest **RhPPO** is dramatically more toxic in MMR− cells, however comparing CW2 (MMR−, IC50: 9.2 μM) and Colo205 (MMR+, IC50: 63 nM) would suggest the opposite trend, with **RhPPO** being dramatically less toxic in MMR− cells. Overall, we believe the large range of IC50 values observed here serves as a point of caution for researchers performing in vitro studies in a limited number of cell lines. Cell line selection can unintentionally but dramatically influence the trends a researcher observes in their studies, therefore we encourage researchers to perform these studies with larger panels of cell lines and to supplement them using matched cell lines, which reduce the inter-cell line variation and allow one to observe the effect of a therapeutic on a specific target.

In summary, the experiments described here underscore the therapeutic and diagnostic potentials of mismatch-targeting small molecules. The potency of **RhPPO** across diverse cell lines spans nearly three orders of magnitude and shows selectivity towards MMR-deficient cancer cells. **RhPPO** is on average 5 times more potent than cisplatin, despite having a less abundant target to which it binds non-covalently. Overall, these results show **RhPPO** is a potent and promising therapeutic agent for colorectal cancers, and in vivo experiments involving mouse models are in progress. Significantly, the fluorescent probe **RhCy3** provides

clear evidence that destabilized DNA regions, such as mismatches, represent the cellular target for the metalloinsertors, and that targeting these lesions leads to cell death. As such, **RhCy3** opens up great perspectives for development of new methods in direct detection and fast quantification of destabilized lesions in genomic DNA and as a fluorescent diagnostic tool for MMR deficient cancers.

Experimental Section

Materials. All commercially available reagents were used as received. The metalloinsertors [Rh(phen)(chrysi)(PPO)]Cl_2 (**RhPPO**) and **RhCy3** were synthesized and purified following published protocols.[12,25] Cell culture media, supplements, and PureLink™ Genomic DNA Mini Kits were purchased from Life Technologies (Carlsbad, CA). CellTiter-Glo® Luminescent Cell Viability Assay kits were purchased from Promega (Madison, WI). BCA Protein Assay Kits were purchased from Pierce (Waltham, MA). Cell lines used in the experiment were purchased from ATCC (Manassas,VA) or provided by collaborators at AMGEN (Thousand Oaks, CA).

Cell Culture. The specific growth conditions of each cell line, including the type of medium and added supplements, can be found in Table S1. In general, cell lines were grown in RPMI 1640, DMEM, McCoy's 5A, or Ham's F-12K media supplemented with 10% FBS (20% FBS for the cell line CaCo2), 100 units/mL penicillin, 100 units/mL streptomycin. Cells were grown in tissue culture treated flasks at 37 °C under a humidified 5% CO2 atmosphere.

CellTiter-Glo Viability Assay. CellTiter-Glo Luminescent Cell Viability Assays were performed following the protocols provided in the kit. Briefly, cell lines were plated at a density of 10,000 cells in 100 µL media per well in an opaque, tissue culture treated 96-well plate and allowed to adhere for 24 h. One of two compounds, **RhPPO** or cisplatin, was added to each well at a final concentration of 0-150 µM, and the cells were allowed to incubate with the therapeutic for 72 h. After incubation with a therapeutic agent, the cell solutions were treated with an equal volume of the CellTiter Glo reagent, which contains beetle luciferin and a recombinant luciferase. The luciferase can catalyze a reaction between the luciferin and ATP provided by viable cells to produce a luminescence that is proportional to the number of viable cells. Luminescence was recorded on a FlexStation 3 Multi-Mode Plate Reader with integration time of 0.500 seconds. Percent viability was determined by the ratio of the luminescence of therapeutic-treated cells compared to untreated cells. IC50 values were determined by fitting the cell viability curve to a sigmoidal curve in OriginPro v 8.5 and using the resultant parameters to calculate the concentration at which 50% of cells were viable. Each therapeutic dose was performed in triplicate and each experiment was repeated 2-3 times to confirm reproducible viability curves. For statistical analyses, cell lines from a common patient (DLD-1/HCT15, HT29/WiDr, SW480/SW620) were averaged and counted as a single cell line to avoid double-counting cancer from a single patient.

ICP-MS Assay for Whole Cell Uptake of RhPPO. Whole cell uptake experiments were performed following previously published protocols with slight modifications.[13] Briefly, cells were plated at a density of 1,000,000 cells in 3 mL media per well in a 6-well plate and allowed to adhere for 24 h. Cells were then treated with **RhPPO** to a final concentration of 0.5 µM. This concentration was selected to be great enough to ensure Rh detection by ICP-MS, but low enough to avoid significant cell death in sensitive cell lines (which could lead to challenges in data analysis). Cells were allowed to incubate for 24 h with the metalloinsertor, as we had previously observed that metalloinsertor uptake plateaus in both HCT116N and HCT116O cells by 24 h.[13] For adherent cell lines, the rhodium-containing medium was aspirated from each well after 24 h and each well was washed 2x with 1 mL of phosphate-buffered saline (PBS) then harvested by trypsinization and transferred to centrifuge tubes. For mixed or suspended cell lines, the rhodium-containing medium was transferred to a centrifuge tube before the PBS rinses and trypsinization. Harvested cells were centrifuged at 1500 rpm for 5 minutes. The supernatant was decanted and the cell pellet was suspended in 1 mL PBS. Centrifugation and PBS washing was repeated three times total (for mixed/suspension cell lines, the suspended and trypsinized aliquots were combined during the second wash). An aliquot from the final suspension was reserved and analyzed for protein content using a Pierce BCA Protein Assay Kit following the manufacturers instructions. To lyse the cells and destroy membrane integrity, each cell suspension was sonicated for 20 s at 40% amplitude on a Qsonica Ultrasonic sonicator, then frozen and lyophilized for 72 h. The resulting cell particulate was suspending in 1 mL of 6% nitric acid and heated at 110 °C for 8 h to facilitate total digestion prior to ICP-MS analysis. Each sample was then diluted to 2% nitric acid and centrifuged to separate any undigested cell components. The solutions were analyzed for Rh content on an Agilent 8800 Triple Quadrupole ICP-MS. The concentration of Rh in each sample was determined by comparison to a standard curve ranging from 0.01 to 100 ppb. Rh concentrations were normalized to the protein content of each sample determined by BCA assay. The measurements were repeated two times using two biological replicates for each cancer cell line.

Genomic DNA extraction and purification. The genomic DNA was extracted and purified using PureLink® Genomic DNA Kits following the manufacturer's protocol. Prior to DNA extraction, the cells subjected to genomic DNA extraction were seeded and grown in their respective cellular medium at < 5 x 10^6 cells/mL. The lysates were prepared by removing the growth medium from the culture plate and cells were harvested by trypsinization then re-suspended in 200 µL PBS. ProteinaseK (20 µL) and RNase (20 µL) were added to the sample, mixed by vortexing and incubated at room temperature for 2 min. 200 µL of PureLink® Genomic Lysis/Binding Buffer were added, mixed and vortexed to obtain a homogenous solution. The samples were incubated at 55 °C for 10 min to promote digestion then 200 µL of 96-100% ethanol was added to the lysate which was further mixed by vortexing for 5 s. The DNA was washed by adding 500 µL of Wash Buffer 1 then Wash Buffer 2 provided by the kit, followed by DNA eluting process using the spin columns. The spin columns were eluted with sterile MilliQ water (200µl) two times to recover a maximum of genomic DNA. The samples were lyophilized and the dry DNA was solubilized in Tris buffer solution (5 mM Tris, 50 mM NaCl, pH = 8.0) in order to obtain a highly concentrated solution. The concentration of gDNA solutions were determined using a NanoDrop 2000 Spectrophotometer (Thermo Scientific) by pippeting 2 µL of the sample solution. The samples purities were determined by obtaining the absorbance ratios at A260/A280 nm and A230/A260 nm using a NanoDrop 2000 Spectrophotometer and are reported in Table S3). The concentrations of the stock solutions of gDNA used during the fluorescence titrations were adjusted at 3140 ng/µl (4.7 mM base pairs DNA) in Tris buffer (200 mM NaCl, 5 mM Tris, pH 8.1).

Fluorescence titrations with genomic DNA. Luminescence spectra were recorded using a QE Pro High Performance Spectrometer with a back-thinned, TE-cooled CCD detector controlled by the OceanView data acquisition and analysis software package (Ocean Optics, Inc.). Sample excitation was provided by a 455 nm LED (Thorlabs model M455L2). The fluorescence titrations in this study were performed with genomic DNA extracted from eight cancer cell lines characterized by different phenotypes (HCT116N, HCT116O, HCT116, DLD-1, HEC-1A, SW480, AN3-CA, DU-145). The emission spectra were recorded in Tris buffer solution (5 mM Tris, 200 mM NaCl, pH = 7.4) at 25 °C using a water circulation system. Excitation wavelength was λEx = 455 nm and emission integral was reported after each addition of genomic DNA, as a scalar function from 548 to 675 nm. The measurements were repeated three times using three biological replicates for each cancer cell line.

Acknowledgements

We gratefully acknowledge Dr. Julie Bailis, for providing the cell lines used in this study. We thank NIH and the Moore Foundation for financial support and the Department of Defense for supporting K.M.B. through the National Defense Science & Engineering Graduate Fellowship program.

Keywords: antitumor agents • cellular uptake • DNA recognition • cytotoxicity

[1] (a) I. I. Arzimanoglou, F. Gilbert, H. R. K. Barber *Cancer* **1998**, *82*, 1808-1820. (b) T. A. Kunkel, D. A. Erie, *Annu. Rev. Genet.* **2015**, *49*, 291–313.

[2] (a) J. Guinney, R. Dienstmann, X. Wang, A. De Reyniès, A. Schlicker, C. Soneson, L. Marisa, P. Roepman, G. Nyamundanda, P. Angelino, et al., *Nat. Med.* **2015**, *21*, 1350–1356. (b) S. B. Hatch, H. M. Lightfoot Jr., C. P. Garwackie, D. T. Moore, B. F. Calvo, J. T. Woosley, J.

Sciarrotta, W. K. Funkhouser, R. A. Farber, *Clin. Can. Res.*, **2005**, *11*, 2180-2187

[3] (a) S. K. Fung, T. Zou, B. Cao, T. Chen, W.-P. To, C. Yang, C.-N. Lok, C.-M. Che, *Nat. Comm.* **2016**, *7*, 10655. (b) A. Granzhan, N. Kotera, M.-P. Teulade-Fichou, *Chem. Soc. Rev.*, **2014**, 42, 3630-3665.

[4] B. A. Jackson, J. K. Barton, *Biochemistry* **2000**, *39*, 6176–6182.

[5] B. A. Jackson, V. Y. Alekseyev, J. K. Barton, *Biochemistry* **1999**, *38*, 4655–4662.

[6] B. M. Zeglis, V. C. Pierre, J. T. Kaiser, J. K. Barton, *Biochemistry* **2009**, *48*, 4247–4253.

[7] B. M. Zeglis, J. A. Boland, J. K. Barton, *Biochemisrty* **2009**, *48*, 839–849.

[8] J. R. Hart, O. Glebov, R. J. Ernst, I. R. Kirsch, J. K. Barton, *Proc. Natl. Acad. Sci.* **2006**, *103*, 15359–15363.

[9] J. M. Bailis, M. L. Gordon, J. L. Gurgel, A. C. Komor, J. K. Barton, I. R. Kirsch, *PLoS One* **2013**, *8*, e78726.

[10] C. Tomasetti, L. Marchionni, M. A. Nowak, G. Parmigiani, B. Vogelstein, *Proc. Natl. Acad. Sci.* **2015**, *112*, 118–123.

[11] I. Martincorena, K. M. Raine, M. Gerstung, K. J. Dawson, K. Haase, P. Van Loo, H. Davies, M. R. Stratton, P. J. Campbell, *Cell* **2017**, *171*, 1029–1041.

[12] A. C. Komor, J. K. Barton, *J. Am. Chem. Soc.* **2014**, *136*, 14160–14172.

[13] K. M. Boyle, J. K. Barton, *J. Am. Chem. Soc.* **2018**, *140*, 5612–5624.

[14] K. C. G. Berg, P. W. Eide, I. A. Eilertsen, B. Johannessen, J. Bruun, S. A. Danielsen, M. Bjørnslett, L. A. Meza-Zepeda, M. Eknæs, G. E. Lind, et al., *Mol. Cancer* **2017**, *16*, 1–16.

[15] J. F. Linnekamp, S. R. Van Hooff, P. R. Prasetyanti, R. Kandimalla, J. Y. Buikhuisen, E. Fessler, P. Ramesh, K. A. S. T. Lee, G. G. W. Bochove, J. H. De Jong, et al., *Cell Death Differ.* **2018**, *25*, 616–633.

[16] M. P. Gleeson, A. Hersey, D. Montanari, J. Overington, *Nat. Rev. Drug Discov.* **2011**, *10*, 197–208.

[17] C. Lipinski, *Am. Pharm. Rev.* **2002**, *5*, 82–85.

[18] J. Mueller, I. Kretzschmar, R. Volkmer, P. Boisguerin, *Bioconjug. Chem.* **2008**, *19*, 2363–2374.

[19] R. Krishna, L. D. Mayer, *Pharm. Pharmacol. Commun.* **1999**, *5*, 511–517.

[20] A. Dayton, K. Selvendiran, M. L. Kuppusamy, B. K. Rivera, S. Meduru, T. Kálai, K. Hideg, P. Kuppusamy, *Cancer Biol. Ther.* **2010**, *10*, 1027–1032.

[21] K. J. Davis, J. A. Carrall, B. Lai, J. R. Aldrich-Wright, S. F. Ralph, C. T. Dillon, *Dalt. Trans.* **2012**, *41*, 9417–9426.

[22] W. E. Glaab, K. R. Tindall, *Carcinogenesis* **1997**, *18*, 1–8.

[23] A. F. El-Yazbi, G. R. Loppnow, *Anal. Chem.* **2013**, *85*, 4321−4327.

[24] H.-W. Liu, L. Chen, C. Xu, Z. Li, H. Zhang, X.-B. Zhang, W. Tan, *Chem. Soc. Rev.* **2018**, *47*, 7140-7180

[25] A. Nano, A. N. Boynton, J. K. Barton, *J. Am. Chem. Soc.* **2017**, *139*, 17301–17304.

[26] J. M. Bailis, A. G. Weidmann, N. F. Mariano, J. K. Barton, *Proc. Natl. Acad. Sci.* **2017**, *114*, 6948–6953.

10.1002/chem.201900042

WILEY-VCH

Entry for the Table of Contents (Please choose one layout)

Layout 2:

COMMUNICATION

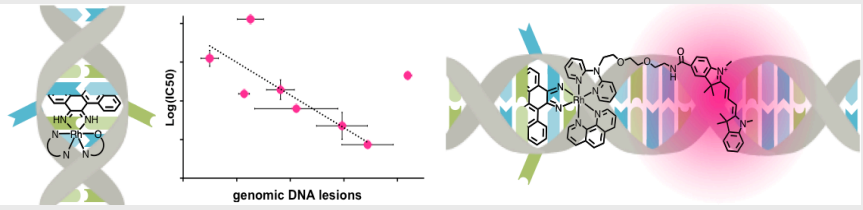

*Kelsey M. Boyle, Adela Nano, Catherine Day, and Jacqueline K. Barton**

Page No. – Page No.

Cellular Target of a Rhodium Metalloinsertor is the DNA Base Pair Mismatch

Targeting DNA Mismatches: Rhodium metalloinsertors are a versatile family of complexes that selectively bind to DNA mismatches in vitro. A range of cytotoxicities is found for the metalloinsertor with higher potency than cisplatin across a panel of colorectal cell lines, and we use a fluorescent analogue to confirm that the DNA mismatch is the primary biological target for the metalloinsertor in cells.